Clonal Evolution Characteristics and Reduced Dimension Prognostic Model for Non-Metastatic Metachronous Bilateral Breast Cancer

Lingyu Li
Jilin University First Hospital
Jiaxuan Li
Jilin University First Hospital
Jiwei Jia
Jilin University
Hua He
Jilin University First Hospital
Mingyang Li
Jilin University
Xu Yan
Jilin University First Hospital
Qing Yu
Geneplus-Beijing
Hanfei Guo
Jilin University First Hospital
Hong Wang
Jilin University First Hospital
Zheng Lv
Jilin University First Hospital
Haishuang Sun
Jilin University First Hospital
Guidong Liao
Jilin University
Jiuwei Cui (cuijw@jlu.edu.cn)
Jilin University First Hospital https://orcid.org/0000-0001-6496-7550

Research article

Keywords: metachronous bilateral breast cancer, SEER database, clonal evolution, nomogram, prognostic evaluation

Posted Date: October 15th, 2021

DOI: https://doi.org/10.21203/rs.3.rs-923832/v1

RESEARCH ARTICLE

Clonal evolution characteristics and reduced dimension prognostic model for non-metastatic metachronous bilateral breast cancer

Lingyu Li[1*], Jiaxuan Li[1*], Jiwei Jia[2,3*], Hua He[1], Mingyang Li[4], Xu Yan[1], Qing Yu[5], Hanfei Guo[1], Hong Wang[1], Zheng Lv[1], Haishuang Sun[1], Guidong Liao[2], Jiuwei Cui[1#]

[*] Lingyu Li, Jiaxuan Li and Jiwei Jia contributed equally to this work.

1. Cancer Center, The First Hospital of Jilin University, 71 Xinmin Street, Changchun, 130021, China
2. School of Mathematics, Jilin University, No. 2699 Qianjin Street, Changchun, 130012, China
3. Jilin National Applied Mathematical Center, Changchun, 130012, China
4. College of Electronic Science and Engineering, Jilin University, No. 2699 Qianjin Street, Changchun, 130012, China
5. Department of Translational Medicine, Geneplus-Beijing, Beijing, 101199, China

[#] Corresponding author:
Jiuwei Cui
Cancer Center, The First Hospital of Jilin University,
No. 71. Xinmin Street, Changchun, 130021
Tel: 86-43188782178 **Fax:** 86-43188786134 **Email:** cuijw@jlu.edu.cn

Abstract

Background:
How to evaluate the prognosis and develop overall treatment strategies of metachronous bilateral breast cancer (MBBC) remains confused in clinical practice.

Methods:
Data from Surveillance, Epidemiology, and End Results (SEER) database and the first hospital of Jilin university were analyzed for breast cancer-specific cumulative mortality (BCCM) by competing risk model. Whole-exome sequencing was applied for 10 lesions acquired at spatial-temporal distinct regions from 5 patients to reconstruct clonal evolutionary characteristics of MBBC. Dimensional reduction (DR) cumulative incidence function (CIF) curves of MBBC features were established on different point in diagnostic interval time, to build a novel DR nomogram.

Results:
Significant heterogeneity in genome and clinical features of MBBC was widespread. The mutational diversity of contralateral BC (CBC) was significantly higher than that in primary BC (PBC), and the most effective prognostic MATH ratio was significantly correlated with interval time (R^2=0.85, $p < .05$). In SEER cohort study (n=13304), the interval time was not only significantly affected the BCCM by multivariate analysis ($p < .000$), but determined the weight of clinical features (T/N stage, grade and ER status) on PBC and CBC in prognostic evaluation. Thus, clinical parameters after DR based on interval time were incorporated into the nomogram for prognostic predicting BCCM. Concordance index was 0.773 (95% CI, 0.769 to 0.776) in training cohort (n=8869), and 0.819 (95% CI, 0.813 to 0.826) in validation cohort (n=4435).

Conclusions:
Bilateral heterogeneous characteristics and interval time were determinant prognostic factors of MBBC. The DR nomogram may help clinical prognostic evaluation.

Keywords:
metachronous bilateral breast cancer, SEER database, clonal evolution, nomogram, prognostic evaluation

Background

Metachronous bilateral breast cancer (MBBC) with high heterogeneity, accounting for 3% of total breast cancer (BC) (1, 2). Owing to the increasing morbidity of BC, prolongation of survival time and improvement of detection rate, a growing number of patients with BC are diagnosed as contralateral disease (2, 3). Recently, majority of studies focused on risk factors for the formation of contralateral breast cancer (CBC) in patients with primary breast cancer (PBC) (4, 35-42), and expected to prevent the occurrence of CBC via bilateral mastectomy (5, 6). While for clinical practice, it is not yet clear whether patients would benefit from bilateral mastectomy in terms of mortality (5). More importantly, once diagnosed as CBC, how to develop overall treatment strategies and evaluate the prognosis of these MBBC remains confused in clinical (7-10, 32). Actually, most clinical understanding of MBBC is obviously distinct from unilateral breast cancer (UBC) (11, 12), and it is urgently needed to build an evaluation model for predicting the prognosis of MBBC.

The spatial-temporal heterogeneity (13) between PBC and CBC, in terms of the clinical, molecular and genomic characteristics (14, 33, 34), makes it more complicated and confused to fully understand this disease (43, 44). In this study, we investigated the regularity of heterogeneity distribution and clonal evolution characteristics between PBC and CBC, and firstly found that the interval time dimension was a determinant prognostic factor of MBBC. Then, we established a novel competing risk model with dimensional reduction (DR) depended on interval time, which may help clinicians in clinical prognostic evaluation and decision making (31, 45).

Methods

Study Population

We obtained the study participants from the population-based Surveillance, Epidemiology, and End Results (SEER) database (1990-2015) and the First Hospital of Jilin University (2001-2019). With a focus on evaluation of MBBC, we defined survivors of CBC as patients with BBC who survived more than 6 months after the diagnosis of PBC (5). While, fulfilling any one of the following criterions would be excluded: (1) had distant metastases at diagnosis of the primary lesion; (2) less than 18 years of age or older than 97 years of age at diagnosis with PBC; (3) The duration of follow-up was less than 3 months or withdraw. Finally, we identified 13304 patients who diagnosed with MBBC between 1990 and 2015. Since human epidermal growth factor receptor 2 (HER2) status was unavailable in SEER before 2010, only 476 patients had recordings of HER2 status. Here, we included patients without distant metastases at first diagnosis to minimize the risk of misclassified metastatic disease.

Whole-exome sequencing and data analysis

Surgically removed sample acquired at spatial-temporal distinct regions from 5 patients with received chemotherapy. DNA libraries for WGS were generated by Illumina TruSeq DNA Library Preparation Kit (Illumina, San Diego, CA) from shear DNA fragments with a peak of 250 bps, which extracted from tumor tissues (the QIAamp DNA FFPE Tissue Kit, Qiagen, Hilden, Germany). NimbleGen EZ 64M

human exome array probes (SeqCap EZ Human Exome Library v3.0) were used in hybridization. DNA sequencing was performed using an HiSeq 3000 instrument (Illumina, San Diego, CA) with 2 x 75 bp paired-end sequencing strategy. Process of reads alignment, calling for somatic single-nucleotide variations (SNVs) are described in the Supplement Data.

Dimensional reduction mathematical model

After plotting cumulative incidence function (CIF) curves of T stage, N stage, grade and ER status at different point in interval time by univariate competing risk analysis, the area under the curve of each subgroup was obtained. According to the difference of the areas among subgroups of the variable, the weight used to evaluate the different proportion of PBC and CBC in predicting the cancer-specific death was calculated at a point in time (15, 16). A reference index of the weight of primary or contralateral cancer was normalized and standardized as the reference weight value of each point in interval time (17). To fit the weight values, the nonlinear fitting function with parameters was set and the regression coefficients were worked out.

Statistical Analysis

Competing risk modeling: Follow-up was begun from the diagnosis of CBC to the date of death or the last recording from SEER or the hospital. In SEER cohort, there were 2357 patients died from cancer and 2624 patients died for other causes within 25 years of follow-up, which was suitable for breast cancer-specific cumulative mortality (BCCM) calculated by Fine and Gray's competing risk model (8) to remove interference from other causes of death. We did not censored follow-up at age more than 70 years since other cause deaths could be excluded by the risk-competitive model.

Construction of the Nomogram: According to the competing risk model, four independent prognostic variables were included and revised by DR mathematical model. We further screened for prognosis impact factors by Fine and Gray's competing risk regression analysis and constructed a corresponding competing risk nomogram. Concordance index (c-index) values were used to measure the discrimination performance and calibration curves were assessed graphically by plotting the observed rates against the nomogram-predicted probabilities via a bootstrap method with 1000 resamples.

Statistics of clinical characteristics between PBC and CBC were analyzed by x2 test used to compare categorical characteristics. In the competing risk model, the clinicopathologic factors affecting the follow-up outcomes independently were selected, subdistribution hazard ratios (SHRs) with 95% confidence interval (CI) were calculated and CIF curves were plotting using STATA Version 15.0. Other data analyses were performed using R software version 3.6.1 (R Foundation for Statistical Computing). Two-sided p value < 0.05 was considered statistically significant.

Results

Clinical characteristics distribution of MBBC

Among 473909 patients with BC in SEER, 13304 individuals of MBBC were

included, which is consistent with a 3%~4% overall morbidity of MBBC (baseline characteristics in Table S1-2). Diagnosis of PBC had a peak at approximately age ranged from 48 to 68 years, and incidence of most CBC were at the ages 56 to 76 years (Fig. 1A-B). The mean age of diagnosis with PBC and CBC was 58 vs. 66 years, and the interval time between PBC and CBC ranged from 6 months to 25 years (mean interval, 7 years), and the occurrence risk of CBC gradually decreased as the time interval lengthens (Fig. 1D). Besides, the younger the onset age of CBC means the shorter spacing interval of MBBC that the median interval in patients younger than 40 years was only 3 years ($p< .0001$, Fig. 1E).

All of the clinical characteristics between PBC and CBC were significantly different, including marriage status, differentiation grade, pathology, tumor size, lymph nodes metastasis (LNM), estrogen receptor (ER) status, progestrone receptor (PR) status and HER2 status ($p< .0001$, Table S3). Heterogeneity of MBBC was obvious in clinical features, inconsistent proportions between PBC and CBC among the above characteristics were 17.14%, 55.77%, 42.64%, 40.11%, 38.18%, 27.50%,38.08% and 22.02%, respectively (Fig. 1C).

Heterogeneity of somatic mutations and clonal evolution in BBC

To evaluate the heterogeneity of nonsilent mutations between bilateral tumor lesion, we sequenced 10 spatially distinct regions from 5 operable patients with BBC. In terms of a single patient, each mutation defined as ubiquitous (present in bilateral tumor regions) or heterogeneous (present in one side of the lesion). Spatial heterogeneity was identified in all five BBCs, with almost all heterogeneous mutations between bilateral tumor lesion (range 95.4% to 100%), except for only one ubiquitous mutation GATA3 in patient P03 (Fig. 2A).

To further explore the dynamics of the mutational processes shaping BBC genomes over time, the spectra of point mutations in each lesion were dissected. Compared with synchronous BBC (patient P01, P02), heterogeneous distribution of somatic mutations in MBBC was significantly associated with the sequence of onset and interval time. The mutational diversity of CBC was significantly higher than that of PBC, and the shorter the interval exhibited the increase in somatic mutation of CBC, indicating the poorer prognosis (patient P03-P05, Fig. 2B).To characterize the genomic instability process between the occurrence of PBC and CBC, we investigated common mutational signatures via catalogue of somatic mutation in cancer (COSMIC[16], https://cancer.sanger.ac.uk/cosmic/signatures_v2), which contained signature1, 6, 11 and 19. Thereinto, signature 1 and 11 were closely associated with age of cancer diagnosis and chemotherapy drugs, such as alkylating agent (Fig. 2C).

To further predict the clinical outcomes of MBBC, we integrated clinical, molecular and ITH (22) features (measured as the percentage of late mutations (23), highlighted the complex interaction between driver status and tumor heterogeneity (24)) from multiple layers, and discovered that several highly correlated features were found to stratify patient outcomes, such as MATH (25) ratio and clone numbers (Fig.S1B). Plotting the correlation structure across these features, we discovered that clinical feature interval time was significantly associated with MATH ratio ($p< .05$, $R^2=0.85$,

Fig.2D-E), suggesting that time interval between BBC is an important reflection of tumor evolution and clinical prognosis. Furthermore, previous large scale sequencing of pan-cancer studies had reported that patient outcome could be better predicted by clinical features than by genomic features (26). Thus, a prognostic model based on essential clinical features might stratify the prognosis of MBBC.

Comprehensive analysis of PBC and CBC in competitive risk model

In our study, to identify the essential features, several clinical parameters were included into competing risk models: 1) race, the age at diagnose time of CBC, the interval time ranged from PBC to CBC; 2) differences of marriage status, tumor size, LNM, grade, pathology, molecular status and surgery types in PBC and CBC. In univariate analysis of BCCM, almost all of the clinical parameters had significant differences ($p < .000$) but for race, marital status and HER2 status. According to multivariate analysis, interval time ($p < .000$), tumor size ($p < .001$), LNM ($p < .006$), grade ($p < .032$) and ER status ($p = 0.006$) between PBC and CBC significantly affected the prognosis of these patients (Table 1, Table S4).

Interval time determines the weight of MBBC characteristics in BCCM

In view of the importance of interval time in tumor clonal evolution, we conducted further stratified analysis at different intervals based on the above prognostic factors. Estimates for BCCM differed across the interval time, significantly survival discrepancy for MBBC patients with spacing interval < 3 years,3-7 years and > 7 years. When patients diagnosed with CBC within 3 years, critical clinical features (T stage, N stage, grade, ER status) of PBC and CBC almost simultaneously inflected the BCCM of patients. Once patients with interval time > 7 years, clinical characteristics in CBC had a prominent impact on the prognosis of these patients, suggesting that interval time might determine the weight of clinical features on PBC and CBC in prognosis evaluation. While for patients with interval time within 3-7 years, the distribution of clinical features was between the above two subgroups (Fig. 3).

Bilateral characteristic DR model of BC based on interval time

Considering the important role of interval time in MBBC and the interference of interphase with other clinical factors on prognosis assessment, we illustrate the DR model dependent on interval time. Taking the T stage as an example (Fig. 4A), we introduce a comprehensive indicator/index to describe the correlation between the bilateral staging:

$$T^{CI} = w_c(t)T^c + w_p(t)T^p$$

Where $w_c(t), w_p(t)$ represent the incidence interval t dependent weighting function, which can be estimated by data fitting. We draw the CIF curve f_{ij} of T stage with respect to interval, by univariate competing risk analysis (PBC defined as i, CBC defined as j), then calculate the L^1 norm of f_{ij} for each subgroup

$$S_{ij} = \int_0^R f_{ij}(\tau)\, d\tau$$

For each interval t, we define the L^1norm difference among all the subgroups as D_p,

$$D_p = \sum_j max\left|S_{i_1 j} - S_{i_2 j}\right|,\ \ i_1 \neq i_2 \circ$$

Normalizing all the D_p, and define it as the (PBC) weight w_p for each interval t. By nonlinear fitting, we obtain the relationship between w_p and t,

$$w_p = a(\frac{\pi}{2} - arctan(\,bt + c)),$$

where a, b and c are the coefficients. Then the weight for (CBC) is defined as

$$w_c = 1 - w_p.$$

On this basis, we employed the same procedure to deal with N stage, tumor cell grade and ER status (Fig. 4B-D).

DR nomogram

According to the DR CIF curve, we reduced the key clinical feature data of PBC and CBC in two times dimensions to the unified dimension and assigned different weights. The weight of T stage on PBC and CBC, for example, a patient with interval of 5 years (T3 stage on PBC and T1 stage on CBC), was 0.37731 and 0.62269, respectively. Ulteriorly, referring to assignment score in table 2, the DR of T stage (T^{DR} stage) =3×0.37731+1×0.62269=1.75462, so T^{DR} stage was II stage (score:1.51-2.0). The DR stage parameters were included in the multivariate analysis of competing risk, T^{DR} ($p < .001$), N^{DR} ($p < .001$), $grade^{DR}$ ($p = .028$), ER^{DR} ($p < .001$), to generate a DR nomogram (Fig. 4E, S1, Table S5). The C-index of the nomogram was 0.773 (95% CI, 0.769 to 0.776) in training cohort (n=8869), and 0.819 (95% CI, 0.813 to 0.826) in validation cohort (n=4435), respectively. Contrast modeling for a single spatial and temporal dimension in previous studies, DR nomogram was proved to have higher predictive power. And calibration plots revealed superb agreement between the nomogram-predicted probabilities and actual observations (Fig. 4F-G).

Discussion

With regard to MBBC, no matter CBC is primary or metastatic, spatial-temporal heterogeneity between the PBC and CBC poses a significant challenge for assessing the prognosis and designing effective treatment regimens (18, 19). However, up to now, no studies have described the heterogeneous distribution and clonal evolution characteristics of these patients with MBBC (27, 28).

In this study, we collected samples and clinical data of BBC at disparate intervals from combined with large sample data from the SEER database, to analyze the clinical heterogeneous features and clonal evolution characteristics of MBBC from time and space dimensions. We verified that significant heterogeneity in genome (Fig.2A) and clinical features (Table.S2) of BBC was widespread, especially for the diversity of driver gene mutation that was almost completely distinct between PBC and CBC. These significant heterogeneity poses a great challenge to the establishment of clinical

prognostic models which just based on unilateral lesion.

More importantly, we found that all of CBCs exhibited more different driver mutations and/or recurrent copy number aberrations than that in PBC, and the mutational diversity of CBC was significantly higher in patients with shorter interval time. Besides, a shorter interval time was significantly associated with a higher MATH ratio and poorer survival, mostly owe to the age of CBC diagnosis (Fig. 1E), chemotherapy drugs (Fig. 2C) and hereditary susceptibility (BRCA1/2 mutations) (26). It all suggested that much shorter an interval often indicated more malignant clonal evolution, and interval time might have a vital influence on outcomes of MBBC.

Just since the time dimension and the weight of clinical features of bilateral lesions was crucial in the prognosis assessment of MBBC (Fig. 3A-D), several previous clinical studies that tried to establish prognostic models based on clinical characteristics, just from one lesion, such as PBC, CBC or worse characteristics (2, 3, 20), could not reflect the real prognosis.

To resolve the issue, we built a bilateral evaluation model that synchronously take heterogeneity of clinical features on both sides of the lesion into account for the first time, including T stage, N stage, grade, ER status and interval time. Even so, the time dimension (interval time), was proven to have complex correlations with the other prognostic factors ($p < .0001$, Fig. 1E, S2), which could interfere with the predictive efficacy of the prognostic model. Thus, we reduced the time dimension dependent on the weight of clinical features of bilateral lesions at distant time node using CIF curves by crossing over with mathematics, to establish DR nomogram for actual observation for 3-, 5-, and 10-year BCCM, which was significantly better optimization of prognosis stratification than a traditional nomogram, and C-index improved by 0.05 and 0.06 in training cohort and internal validation cohort, respectively. Besides, this nomogram was only based on four basic clinical features, which greatly improves the clinical applicability of this model and facilitates clinical popularization. And the application of the dimension reduction method could also extrapolate the prediction model to the clinical prediction of synchronous breast cancer, and only the weight balance of occurrence of bilateral breast cancer is 0.5.

Validation of the nomogram is essential to avoid over-fitting and determine generalizability of prognostic model (29). In the current study, calibration plots showed optimal agreement between prediction and actual observation, guaranteeing the reliability and feasibility of the established nomogram (Fig. 4F-G). The much higher C-index of the DR nomogram was revealed in internal validation cohort than that in the training cohort, indicating the effective repeatability. In the tentative external validation cohort from China (n=89), the C-index was similar with the training cohort, suggested that the model was adaptable to the Asian population in spite of the small sample size.

On the other hand, whole-exome sequencing showed that gene mutations seemed to be completely different in PBC and CBC, hard to pin down the correlations with specific genetic mutations. However, the mutation signatures were all concentrated in the characteristics related to chemotherapeutic drugs alkylating agents, suggesting that the significance of drug stress selection in clone evolution (29, 30). This study provided an excellent in vivo model for improving the understanding of tumor evolution, which

would guide clinical decision-making to a certain extent. For example, the significance of chemotherapy elimination regimen for the malignant evolution of contralateral tumors and long-term outcome in patients with early breast cancer should be considered.

Conclusions

We established and validated a novel DR nomogram for predicting BCCM of patients with MBBC. The clinicians could more precisely estimate the survival of individual patients and identify subgroups of patients who are in need of a specific treatment strategy by this nomogram. However, validation of large sample and multicenter clinical data are still needed in the future.

Declarations

Ethics approval and consent to participate

The protocol was in accordance with the precepts of the Helsinki Declaration and approved by the the Ethics Committee of the First Hospital of Jilin University. The informed consents were obtained from each participant or each participant's guardian.

Consent for publication

The manuscript is not under consideration by any other journal and all authors have contributed to, read and approved the manuscript that is enclosed.

Availability of data and materials

The datasets downloaded from the SEER database are available on their public website. Other datasets generated or analysed during this study are available from the corresponding author on reasonable request.

Competing interests

The authors declare that they have no competing interests.

Funding

This work was supported by Research on Chronic Noncommunicable Diseases Prevention and Control of National Ministry of Science and Technology (2016YFC1303804), National Natural Science Foundation of China grant (81672275, 81874052, 3A214DJ63428) to J. Cui; the Youth Fund of the National Natural Science Foundation of China (81802487) and Youth Development Foundation of the First Hospital of Jilin University (JDYY92018028, 2020-ZL-06) to L. Li.

Author contribution statement

Conception and design: Lingyu Li, Jiuwei Cui
Financial support: Lingyu Li, Jiuwei Cui
Administrative support: Lingyu Li, Jiuwei Cui, Hua He
Provision of study materials or patients: Jiaxuan Li, Hanfei Guo, Hong Wang, Zheng Lv
Collection and assembly of data: Jiaxuan Li, Xu Yan, Haishuang Sun, Hong Wang,

Zheng Lv
Data analysis and interpretation: Lingyu Li, Jiaxuan Li, Jiwei Jia, Mingyang Li, Qing Yu, Guidong Liao
Manuscript writing: Lingyu Li, Jiaxuan Li, Jiwei Jia, Mingyang Li, Qing Yu, Jiuwei Cui
Final approval of manuscript: All authors

Acknowledgements

The authors thank Gang Li, Hongping Song and Wang Yang for their disinterested assistance.

REFERENCES

1. Gong SJ, Rha SY, Jeung HC, Roh JK, Yang WI, Chung HC. Bilateral breast cancer: differential diagnosis using histological and biological parameters. Jpn J Clin Oncol 2007;37:487-92.
2. Kheirelseid EA, Jumustafa H, Miller N, Curran C, Sweeney K, Malone C, et al. Bilateral breast cancer: analysis of incidence, outcome, survival and disease characteristics. Breast Cancer Res Treat 2011;126:131-40.
3. Hartman M, Czene K, Reilly M, Adolfsson J, Bergh J, Adami HO, et al. Incidence and prognosis of synchronous and metachronous bilateral breast cancer. J Clin Oncol 2007;25:4210-6.
4. Figueiredo JC, Bernstein L, Capanu M, Malone KE, Lynch CF, Anton-Culver H, et al. Oral contraceptives, postmenopausal hormones, and risk of asynchronous bilateral breast cancer: the WECARE Study Group. J Clin Oncol 2008;26:1411-8.
5. Narod SA. Bilateral breast cancers. Nat Rev Clin Oncol 2014;11:157-66.
6. Herrinton LJ, Barlow WE, Yu O, Geiger AM, Elmore JG, Barton MB, et al. Efficacy of prophylactic mastectomy in women with unilateral breast cancer: a cancer research network project. J Clin Oncol 2005;23:4275-86.
7. Tsyhyka DY, Hotko YS, Devinyak OT. Receptor status of tumor as prognostic factor in patients with bilateral breast cancer. Exp Oncol 2013;35:291-4.
8. Tong G, Geng Q, Cheng J, Chai J, Xia Y, Feng R, et al. Effects of psycho-behavioral interventions on immune functioning in cancer patients: a systematic review. J Cancer Res Clin Oncol 2014;140:15-33.
9. DeSantis CE, Ma J, Goding Sauer A, Newman LA, Jemal A. Breast cancer statistics, 2017, racial disparity in mortality by state. CA Cancer J Clin 2017;67:439-48.
10. Jobsen JJ, van der Palen J, Brinkhuis M, Ong F, Struikmans H. Long-term effects of first degree family history of breast cancer in young women: Recurrences and bilateral breast cancer. Acta Oncol 2016;55:449-54.
11. Mruthyunjayappa S, Zhang K, Zhang L, Eltoum IA, Siegal GP, Wei S. Synchronous and metachronous bilateral breast cancer: clinicopathologic characteristics and prognostic outcomes. Hum Pathol 2019;92:1-9.
12. Pan B, Xu Y, Zhou YD, Yao R, Wu HW, Zhu QL, et al. The prognostic comparison among unilateral, bilateral, synchronous bilateral, and metachronous bilateral breast cancer: A meta-analysis of studies from recent decade (2008-2018). Cancer Med 2019;8:2908-18.
13. Welch DR. Tumor Heterogeneity--A 'Contemporary Concept' Founded on Historical Insights and Predictions. Cancer Res 2016;76:4-6.
14. Zardavas D, Irrthum A, Swanton C, Piccart M. Clinical management of breast cancer heterogeneity. Nat Rev Clin Oncol 2015;12:381-94.
15. Yosida BK. Functional Analysis :Springer-Verlag;1978.
16. Neumaier A. Introduction to Numerical Analysis: Linear Systems of Equations. 2001.
17. Hiroshi, Akima. A New Method of Interpolation and Smooth Curve Fitting Based on Local Procedures. Journal of the Acm 1970.
18. Ellsworth RE, Blackburn HL, Shriver CD, Soon-Shiong P, Ellsworth DL. Molecular heterogeneity in breast cancer: State of the science and implications for patient care. Semin Cell Dev Biol 2017;64:65-72.
19. Turashvili G, Brogi E. Tumor Heterogeneity in Breast Cancer. Front Med (Lausanne) 2017;4:227.
20. Shen K, Yao L, Wei J, Luo Z, Yu W, Zhai H, et al. Worse characteristics can predict survival effectively in bilateral primary breast cancer: A competing risk nomogram using the SEER database. Cancer Med 2019;8:7890-902.
21. Sondka Z, Bamford S, Cole CG, Ward SA, Dunham I, Forbes SA. The COSMIC Cancer Gene Census:

describing genetic dysfunction across all human cancers. Nat Rev Cancer 2018;18:696-705.

22. Jamal-Hanjani M, Wilson GA, McGranahan N, Birkbak NJ, Watkins T, Veeriah S, et al. Tracking the Evolution of Non-Small-Cell Lung Cancer. N Engl J Med 2017;376:2109-21.

23. McGranahan N, Favero F, de Bruin EC, Birkbak NJ, Szallasi Z, Swanton C. Clonal status of actionable driver events and the timing of mutational processes in cancer evolution. Sci Transl Med 2015;7:283ra54.

24. Nahar R, Zhai W, Zhang T, Takano A, Khng AJ, Lee YY, et al. Elucidating the genomic architecture of Asian EGFR-mutant lung adenocarcinoma through multi-region exome sequencing. Nat Commun 2018;9:216.

25. Mroz EA, Rocco JW. MATH, a novel measure of intratumor genetic heterogeneity, is high in poor-outcome classes of head and neck squamous cell carcinoma. Oral Oncol 2013;49:211-5.

26. Yuan Y, Van Allen EM, Omberg L, Wagle N, Amin-Mansour A, Sokolov A, et al. Assessing the clinical utility of cancer genomic and proteomic data across tumor types. Nat Biotechnol 2014;32:644-52.

27. Ibragimova MK, Tsyganov MM, Litviakov NV. Natural and Chemotherapy-Induced Clonal Evolution of Tumors. Biochemistry (Mosc) 2017;82:413-25.

28. Bowman RL, Busque L, Levine RL. Clonal Hematopoiesis and Evolution to Hematopoietic Malignancies. Cell Stem Cell 2018;22:157-70.

29. Iasonos A, Schrag D, Raj GV, Panageas KS. How to build and interpret a nomogram for cancer prognosis. J Clin Oncol 2008;26:1364-70.

30. Ghoussaini M, Pharoah PD. Polygenic susceptibility to breast cancer: current state-of-the-art. Future Oncol 2009;5:689-701.

31. Posey JT, Soloway MS, Ekici S, Sofer M, Civantos F, Duncan RC, et al. Evaluation of the prognostic potential of hyaluronic acid and hyaluronidase (HYAL1) for prostate cancer. Cancer Res 2003;63:2638-44.

32. Raghavendra A, Sinha AK, Le-Petross HT, Garg N, Hsu L, Patangan M Jr, et al. Mammographic breast density is associated with the development of contralateral breast cancer. Cancer 2017;123:1935-40.

33. ESh K, Grigoriev MY, Suspitsin EN, Buslov KG, Zaitseva OA, Yatsuk OS, et al. Microsatellite instability analysis of bilateral breast tumors suggests treatment-related origin of some contralateral malignancies. J Cancer Res Clin Oncol 2007;133:57-64.

34. Iyevleva AG, ESh K, Mitiushkina NV, Togo AV, Miki Y, Imyanitov EN. High level of miR-21, miR-10b, and miR-31 expression in bilateral vs. unilateral breast carcinomas. Breast Cancer Res Treat 2012;131:1049-59.

35. Langballe R, Cronin-Fenton D, Dehlendorff C, Jensen MB, Ejlertsen B, Andersson M, et al. Statin use and risk of contralateral breast cancer: a nationwide cohort study. Br J Cancer 2018;119:1297-305.

36. Gierach GL, Curtis RE, Pfeiffer RM, Mullooly M, Ntowe EA, Hoover RN, et al. Association of Adjuvant Tamoxifen and Aromatase Inhibitor Therapy With Contralateral Breast Cancer Risk Among US Women With Breast Cancer in a General Community Setting. JAMA Oncol 2017;3:186-93.

37. Alkner S, Bendahl PO, Fernö M, Nordenskjöld B, Rydén L, South Swedish and South-East Swedish Breast Cancer Groups. Tamoxifen reduces the risk of contralateral breast cancer in premenopausal women: Results from a controlled randomised trial. Eur J Cancer 2009;45:2496-502.

38. Kurian AW, Canchola AJ, Ma CS, Clarke CA, Gomez SL. Magnitude of reduction in risk of second contralateral breast cancer with bilateral mastectomy in patients with breast cancer: Data from California, 1998 through 2015. Cancer 2020;126:958-70.

39. Bens A, Langballe R, Bernstein JL, Cronin-Fenton D, Friis S, Mellemkjaer L. Preventive drug therapy and contralateral breast cancer: summary of the evidence of clinical trials and observational studies. Acta Oncol 2019;58:1581-93.

40. Hackshaw A, Roughton M, Forsyth S, Monson K, Reczko K, Sainsbury R, et al. Long-term benefits of 5 years of tamoxifen: 10-year follow-up of a large randomized trial in women at least 50 years of age with

early breast cancer. J Clin Oncol 2011;29:1657-63.

41. Davies C, Pan H, Godwin J, Gray R, Arriagada R, Raina V, et al. Long-term effects of continuing adjuvant tamoxifen to 10 years versus stopping at 5 years after diagnosis of oestrogen receptor-positive breast cancer: ATLAS, a randomised trial. Lancet 2013;381:805-16.

42. Kramer I, Schaapveld M, Oldenburg H, Sonke GS, McCool D, van Leeuwen FE, et al. The Influence of Adjuvant Systemic Regimens on Contralateral Breast Cancer Risk and Receptor Subtype. J Natl Cancer Inst 2019;111:709-18.

43. Mejdahl MK, Wohlfahrt J, Holm M, Balslev E, Knoop AS, Tjønneland A, et al. Breast cancer mortality in synchronous bilateral breast cancer patients. Br J Cancer 2019;120:761-7.

44. Chen R, Goodison S, Sun Y. Molecular Profiles of Matched Primary and Metastatic Tumor Samples Support a Linear Evolutionary Model of Breast Cancer. Cancer Res 2020;80:170-4.

45. Wu L, Ge C, Zheng H, Lin H, Fu W, Fu J. Establishing a Competing Risk Regression Nomogram Model for Survival Data. J Vis Exp 2020.

Table 1. Competing Risk Model for MBBC

Variable	No. of patients	%	Univariate Analysis				Multivariate Analysis			
			P Value	Sub-Distri-bution HR	95% CI low	95% CI upp	*P* Value	Sub-Distri-bution HR	95% CI low	95% CI upp
Age at Diagnosis of CBC (years)										
<=40	411	3.09	Ref				Ref			
41-50	1493	11.22	<0.001	0.66	0.55	0.80	0.229	0.76	0.49	1.19
51-60	2739	20.59	<0.001	0.49	0.41	0.58	0.688	0.92	0.60	1.40
>60	8661	65.10	<0.001	0.36	0.30	0.42	0.738	0.93	0.61	1.42
Interval Time（years）										
Continuous Variable form	13304		<0.001	0.93	0.92	0.94	**<0.001**	**0.92**	**0.89**	**0.95**
<=7	7551	56.76	Ref							
>7	5753	43.24	<0.001	0.56	0.51	0.61				
Race										
White, non-Hispanic	10731	80.68	Ref				Ref			
Black, non-Hispanic	1308	9.83	<0.001	1.63	1.45	1.84	0.383	0.88	0.67	1.17
Other, mixed	1261	9.48	0.542	0.95	0.82	1.11	0.198	1.22	0.90	1.65
Marital Status										
Non-P/Non-P	4371	35.20	Ref				Ref			
Non-P/With-P	382	3.08	0.489	0.91	0.71	1.18	0.732	0.91	0.55	1.53
With-P/Non-P	1304	10.50	0.017	0.83	0.71	0.97	0.240	0.78	0.52	1.18
With-P/Non-P	6359	51.22	0.004	0.88	0.80	0.96	0.181	0.88	0.72	1.06
T Stage										
T1/T1	6069	51.55	Ref				Ref			
T1/T2	1438	12.22	<0.001	2.41	2.09	2.77	**<0.001**	**2.23**	**1.67**	**2.99**
T1/T3-T4	285	2.42	<0.001	6.03	4.89	7.43	**<0.001**	**4.70**	**3.01**	**7.35**
T2/T1	2169	18.43	<0.001	1.92	1.68	2.19	**0.001**	**1.65**	**1.24**	**2.20**
T2/T2	757	6.43	<0.001	3.40	2.89	3.99	**<0.001**	**3.06**	**2.23**	**4.19**
T2/T3-T4	237	2.01	<0.001	8.98	7.16	11.25	**<0.001**	**5.19**	**2.99**	**8.99**
T3-T4/TI	437	3.71	<0.001	3.23	2.63	3.96	**0.001**	**2.28**	**1.42**	**3.67**
T3-T4/T2	197	1.67	<0.001	6.55	5.12	8.38	**<0.001**	**3.30**	**2.03**	**5.37**
T3-T4/T3-T4	183	1.55	<0.001	15.24	12.21	19.02	**<0.001**	**4.25**	**2.38**	**7.57**

(continued on following page)

Table 1. Competing Risk Model for MBBC (continued)

Variable	No. of patients	%	Univariate Analysis				Multivariate Analysis			
			P Value	Sub-Distri-butio n HR	95% CI low	95% CI upp	*P* Value	Sub-Distri-bution HR	95% CI low	95% CI upp
N Stage										
N0/N0	6740	57.22	Ref				Ref			
N0/N1	1236	10.49	<0.001	2.28	1.96	2.65	**<0.001**	**1.76**	**1.29**	**2.40**
N0/N2-N3	499	4.24	<0.001	5.74	4.88	6.75	**<0.001**	**3.60**	**2.49**	**5.21**
N1/N0	1620	13.75	<0.001	1.73	1.49	2.01	**0.006**	**1.51**	**1.13**	**2.03**
N1/N1	404	3.43	<0.001	4.00	3.28	4.87	**<0.001**	**3.46**	**2.42**	**4.94**
N1/N2-N3	230	1.95	<0.001	9.41	7.75	11.43	**<0.001**	**4.58**	**3.07**	**6.84**
N2-N3/N0	615	5.22	<0.001	3.59	3.03	4.25	**<0.001**	**3.24**	**2.24**	**4.68**
N2-N3/N1	194	1.65	<0.001	6.29	4.97	7.97	**<0.001**	**4.10**	**2.45**	**6.87**
N2-N3/N2-N3	241	2.05	<0.001	14.51	12.09	17.41	**<0.001**	**6.14**	**3.82**	**9.88**
Tumor Grade										
I-II/I-II	4738	45.58	Ref				Ref			
I-II/III-IV	1562	15.03	<0.001	2.05	1.78	2.35	**0.032**	**1.34**	**1.02**	**1.76**
III-IV/I-II	1998	19.22	<0.001	1.32	1.14	1.52	0.338	1.15	0.86	1.55
III-IV/III-IV	2098	20.18	<0.001	2.80	2.49	3.15	**0.001**	**1.63**	**1.23**	**2.16**
Pathological Type										
IDC/IDC	6841	51.42	Ref				Ref			
IDC/ILC	825	6.20	0.727	0.97	0.81	1.16	0.813	0.95	0.61	1.48
IDC/Other	1686	12.67	0.384	1.06	0.93	1.20	0.356	1.15	0.86	1.54
ILC/IDC	536	4.03	0.477	0.93	0.75	1.15	0.860	1.05	0.60	1.86
ILC/ILC	278	2.09	<0.001	1.74	1.38	2.19	0.220	1.41	0.81	2.45
ILC/Other	177	1.33	0.133	1.26	0.93	1.70	0.717	1.13	0.59	2.15
Other/IDC	1909	14.35	0.731	1.02	0.91	1.15	**0.011**	**1.40**	**1.08**	**1.81**
Other/ILC	313	2.35	0.785	1.04	0.79	1.38	0.257	1.35	0.81	2.25
Other/Other	739	5.55	0.158	1.13	0.95	1.35	0.187	1.30	0.88	1.90
Surgery Method										
BCM/BCM	2699	42.24	Ref				Ref			
BCM/SM	814	12.74	0.520	1.09	0.83	1.43	0.630	0.92	0.66	1.28
BCM/RM	541	8.47	<0.001	2.25	1.80	2.83	0.708	0.94	0.69	1.29

(continued on following page)

Table 1. Competing Risk Model for MBBC (continued)

Variable	No. of patients	%	Univariate Analysis				Multivariate Analysis			
			P Value	Sub-Distri-bution HR	95% CI low	95% CI upp	*P* Value	Sub-Distri-bution HR	95% CI low	95% CI upp
SM/BCM	124	1.94	0.073	1.59	0.96	2.65	0.902	0.95	0.45	2.03
SM/SM	332	5.20	0.353	0.81	0.52	1.26	**0.015**	**0.48**	**0.27**	**0.87**
SM/RM	154	2.41	<0.001	2.41	1.67	3.49	0.922	0.98	0.60	1.60
RM/BCM	330	5.17	<0.001	2.09	1.56	2.78	0.685	0.92	0.60	1.41
RM/SM	619	9.69	<0.001	1.59	1.23	2.06	0.580	0.91	0.64	1.28
RM/SM	776	12.15	<0.001	2.87	2.38	3.46	0.456	0.90	0.68	1.19
ER Status										
+/+	6286	61.02	Ref				Ref			
+/-	1279	12.42	<0.001	1.73	1.51	1.98	0.060	1.29	0.99	1.68
-/+	1480	14.37	0.685	0.97	0.83	1.13	**0.006**	**0.64**	**0.46**	**0.88**
-/-	1256	12.19	<0.001	2.19	1.93	2.50	0.103	1.28	0.95	1.72
PR Status										
+/+	4290	43.49	Ref							
+/-	2213	22.44	<0.001	1.69	1.49	1.91				
-/+	1592	16.14	0.738	0.97	0.82	1.15				
-/-	1769	17.93	<0.001	2.07	1.82	2.36				
HER2 Status										
+/+	23	4.83	Ref							
+/-	26	5.46	<0.001	0.00	0.00	0.00				
-/+	54	11.34	0.309	0.38	0.06	2.42				
-/-	373	78.36	0.454	0.57	0.13	2.46				

Abbreviations: MBBC, metachronous bilateral breast cancer; No., number; Sub-Distribution HR, subdistribution hazard ratio; CI, confidence interval; low, lower bound of confidence interval; upp, upper bound of confidence interval; CBC, contralateral breast cancer; Ref, reference; Non-P, without partner at diagnosis (single, divorced, widowed, separated); With-P, with partner at diagnosis (married, unmarried or domestic partner, same sex or opposite sex partner); T, tumor; N: node; IDC, invasive ductal carcinoma; ILC, invasive lobular carcinoma; BCS, breast-conserving surgery; SM, simple mastectomy; RM, radical mastectomy; ER, estrogen receptor; PR, progesterone receptor; HER2, human epidermal growth factor receptor 2; +, positive; -, negative.

Table 2. Prognostic Score Assignment and DR Algorithm

Variable	Score of PBC	Score of CBC	Total Score (Range)	Cutoff Value of Total Score	DR Stage
T Stage			(1.00~3.00)		**T^{DR} Stage**
T1/T1	1	1	=1*Wpt+1*Wct	1.00~1.50	1
T1/T2	1	2	=1*Wpt+2*Wct	1.51~2.00	2
T1/T3-T4	1	3	=1*Wpt+3*Wct	2.01~2.50	3
T2/T1	2	1	=2*Wpt+1*Wct	2.51~3.00	4
T2/T2	2	2	=2*Wpt+2*Wct		
T2/T3-T4	2	3	=2*Wpt+3*Wct		
T3-T4/TI	3	1	=3*Wpt+1*Wct		
T3-T4/T2	3	2	=3*Wpt+2*Wct		
T3-T4/T3-T4	3	3	=3*Wpt+3*Wct		
N Stage			(1.00~3.00)		**N^{DR} Stage**
N1/N1	1	1	=1*Wpn+1*Wcn	1.00~1.50	1
N1/N2	1	2	=1*Wpn+2*Wcn	1.51~2.00	2
N1/N3-N4	1	3	=1*Wpn+3*Wcn	2.01~2.50	3
N2/N1	2	1	=2*Wpn+1*Wcn	2.51~3.00	4
N2/N2	2	2	=2*Wpn+2*Wcn		
N2/N3-N4	2	3	=2*Wpn+3*Wcn		
N3/N1	3	1	=3*Wpn+1*Wcn		
N3/N2	3	2	=3*Wpn+2*Wcn		
N3/N3-N4	3	3	=3*Wpn+3*Wcn		
Grade			(1.00~2.00)		**$Grade^{DR}$**
I-II/I-II	1	1	=1*Wpg+1*Wcg	1.00~1.50	1
I-II/III-IV	1	2	=1*Wpg+2*Wcg	1.51~2.00	2
III-IV/I-II	2	1	=2*Wpg+1*Wcg		
III-IV/III-IV	2	2	=2*Wpg+2*Wcg		
ER Status			(1.00~2.00)		**ER^{DR} Status**
+/+	1	1	=1*Wpe+1*Wce	1.00~1.50	1
+/-	1	2	=1*Wpe+2*Wce	1.51~2.00	2
-/+	2	1	=2*Wpe+1*Wce		
-/-	2	2	=2*Wpe+2*Wce		

Abbreviations: DR: dimension reduction; Wpt, weight of PBC's T stage for prognostic prediction; Wct, weight of CBC's T stage for prognostic prediction; Wpn, weight of PBC's N stage for prognostic prediction; Wct, weight of CBC's N stage for prognostic prediction; Wpg, weight of PBC's grade for prognostic prediction; Wcg, weight of CBC's grade for prognostic prediction; Wpe, weight of PBC's ER status for prognostic prediction; Wce, weight of CBC's ER status for prognostic prediction.

LEGENDS

Figure 1. Distribution of clinical characters in MBBC from SEER

(A-B) Age distribution in MBBC: the number of patients plotted on the y-axis against age on the x-axis for PBC (A) and CBC (B). The mean age of diagnosis with PBC and CBC was 58 vs. 66 years, respectively.

(C) The consistent radio by different clinical features on the y-axis against gender on the x-axis.

(D) The number of patients with CBC plotted on the y-axis against the interval time, and the mean was 7 years.

(E) Patients were divided into 5 groups according to age at diagnosis of CBC (≤40, 41-50, 51-60, 61-70, ≥71), the range of interval time was counted on the x-axis.

Figure 2. Heterogeneity of somatic mutations and clonal evolution in BBC

(A) Heat maps show the clinical characters and individual somatic mutations of 5 BBC patients with different interval time (rang from less than 6 months to 61 months) in right breast (orange) and left breast (green) of SBBC (P01,P02), or PBC (blue) and CBC (yellow) of MBBC. The presence (blue) or absence (gray) of each mutation is indicated for every tumor region. Clonal evolution of 10 pathological specimens after operation (L001 to L019) from different spatial regions.

(B) Fraction of early mutations (trunk) and late mutations (branch) accounted for by each of the six mutation types in all samples.Driver mutations occurring in an APOBEC signature (C>T and C>G mutations) are highlighted with blue and yellow box.

(C) Heat maps show the common mutational signatures via COSMIC.

(D) The total importance for each feature group.

(E) Correlation and prognosis importance for 14 features, including clinical (green points), molecular (purple points) characters and ITH (orange points) was shown by wires. Dark orange wires meant the relevance of each point had statistically significant ($p < .05$) and gray wires meant insignificance ($p > .05$).

(F) The relationship of the interval time and MATH-score-ratio was described by regression equation, y=0.88-0.02x.

Figure 3. Interval time in stratified BCCM of MBBC characteristics

Risk group stratification within each prognostic factor with distant interval time (<3, 3-7, >7 years), including T stage (A), N stage (B), grade (C), and ER status (D).The same features of PBC are reflected with the same line type (solid or dashed line), and the same features of CBC are reflected with the same line color (blue, yellow or gray).

Figure 4. Weight of CIF curves on interval time and DR nomogram

(A-D) The weight of T stage (A), N stage (B), grade (C) and ER status (D) belonging to PBC or CBC for prognostic prediction changed with interval time. CIF curves were created to identify the weight of PBC and CBC of the patient with specific interval time when using each character to predict BCCM. Wp: weight of PBC's character. Wc: weight of CBC's character.

(E) DR prognostic nomogram for patients with MBBC. Competing risk dimensionality reduction nomogram for predicting the 3-, 5-, and 10-year probabilities of breast cancer-specific survival (BCSS).
(F-G) Calibration plots for 3-, 5-, and 10-year probabilities of DR nomogram in the training (F) and validation (G) cohort. The solid line represents equality between the predicted and observed probabilities. With the dots close to the solid line, the plots reveal excellent agreement between the nomogram-predicted probabilities and actual observations.

Supplementary Figure 1. The BCCM curves of DR clinical features in MBBC
BCCM curves plotted by CIF curves of each prognostic factor (T stage, N stage, grade, ER status) after revised to DR clinical feature (T^{DR} stage, N^{DR} stage, $grade^{DR}$, ER^{DR} status) are divided into subgroups according to the score range and reflected with different line color (blue, yellow, gray or orange red).

Supplementary Figure 2. The correlation between interval time and other prognostic features
The range of interval time at each subgroup MBBC patients divided by prognostic features, T stage (A), N stage (B), grade (C), ER status (D) was described, respectively. The median interval time of was compared to reflect the correlation.

Figures

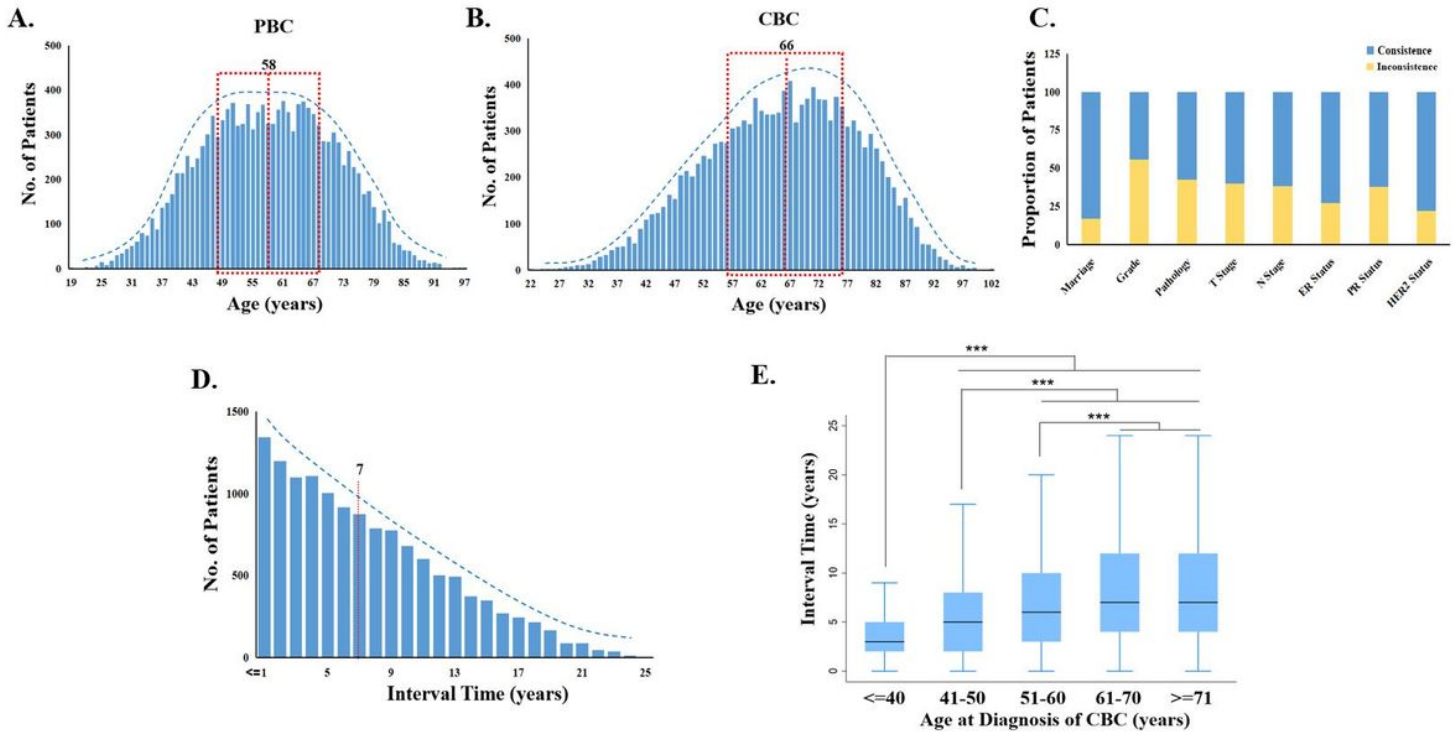

Figure 1

Distribution of clinical characters in MBBC from SEER (A-B) Age distribution in MBBC: the number of patients plotted on the y-axis against age on the x-axis for PBC (A) and CBC (B). The mean age of diagnosis with PBC and CBC was 58 vs. 66 years, respectively. (C) The consistent radio by different clinical features on the y-axis against gender on the x-axis. (D) The number of patients with CBC plotted on the y-axis against the interval time, and the mean was 7 years. (E) Patients were divided into 5 groups according to age at diagnosis of CBC (≤40, 41-50, 51-60, 61-70, ≥71), the range of interval time was counted on the x-axis.

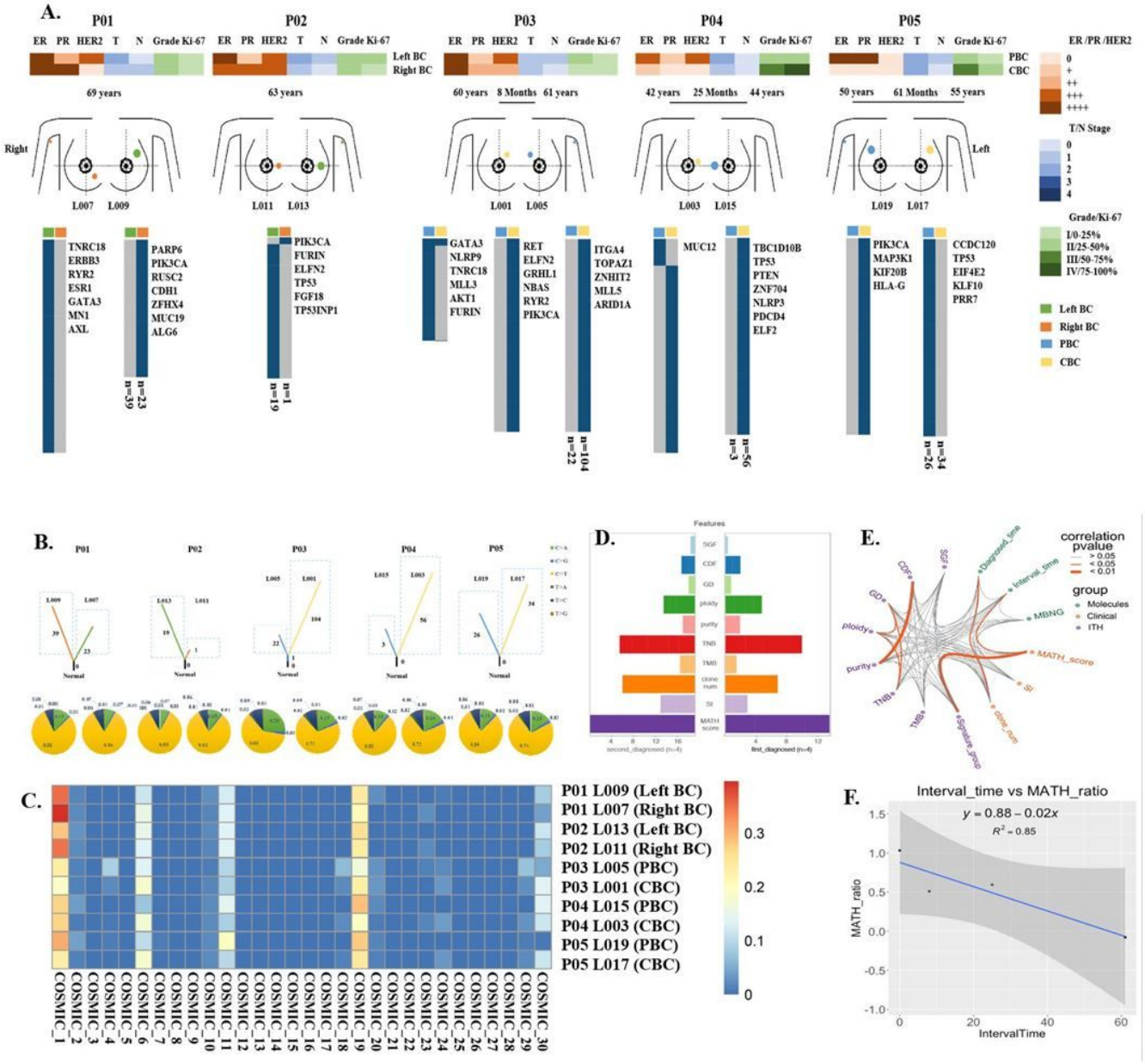

Figure 2

Heterogeneity of somatic mutations and clonal evolution in BBC (A) Heat maps show the clinical characters and individual somatic mutations of 5 BBC patients with different interval time (rang from less than 6 months to 61 months) in right breast (orange) and left breast (green) of SBBC (P01,P02), or PBC (blue) and CBC (yellow) of MBBC. The presence (blue) or absence (gray) of each mutation is indicated for every tumor region. Clonal evolution of 10 pathological specimens after operation (L001 to L019) from different spatial regions. (B) Fraction of early mutations (trunk) and late mutations (branch) accounted for by each of the six mutation types in all samples.Driver mutations occurring in an APOBEC signature (C>T and C>G mutations) are highlighted with blue and yellow box. (C) Heat maps show the common mutational signatures via COSMIC. (D) The total importance for each feature group. (E) Correlation and prognosis importance for 14 features, including clinical (green points), molecular (purple points) characters and ITH (orange points) was shown by wires. Dark orange wires meant the relevance of each

point had statistically significant (p< .05) and gray wires meant insignificance (p> .05). (F) The relationship of the interval time and MATH-score-ratio was described by regression equation, y=0.88-0.02x.

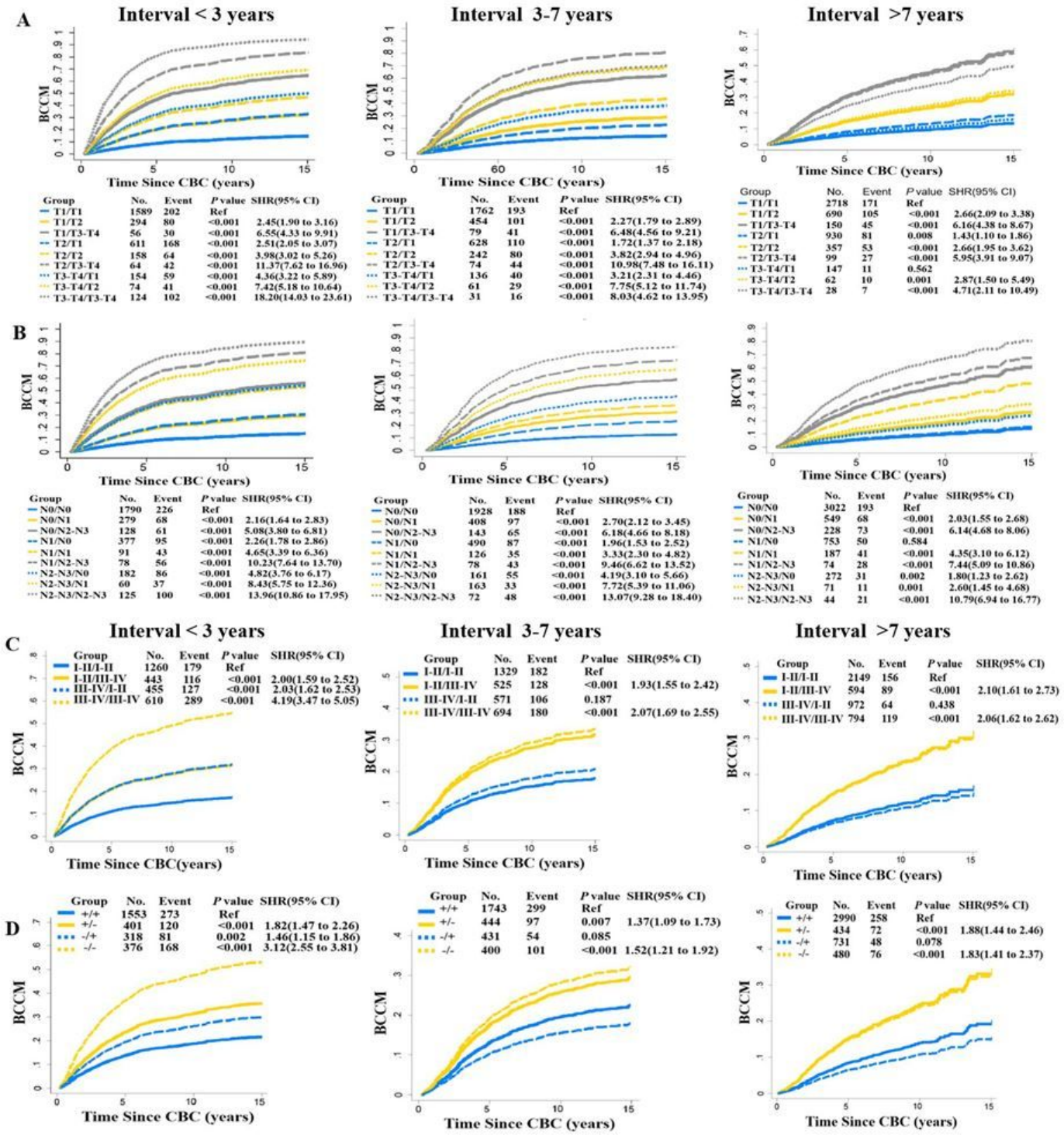

Figure 3

Interval time in stratified BCCM of MBBC characteristics Risk group stratification within each prognostic factor with distant interval time (<3, 3-7, >7 years), including T stage (A), N stage (B), grade (C), and ER

status (D).The same features of PBC are reflected with the same line type (solid or dashed line), and the same features of CBC are reflected with the same line color (blue, yellow or gray).

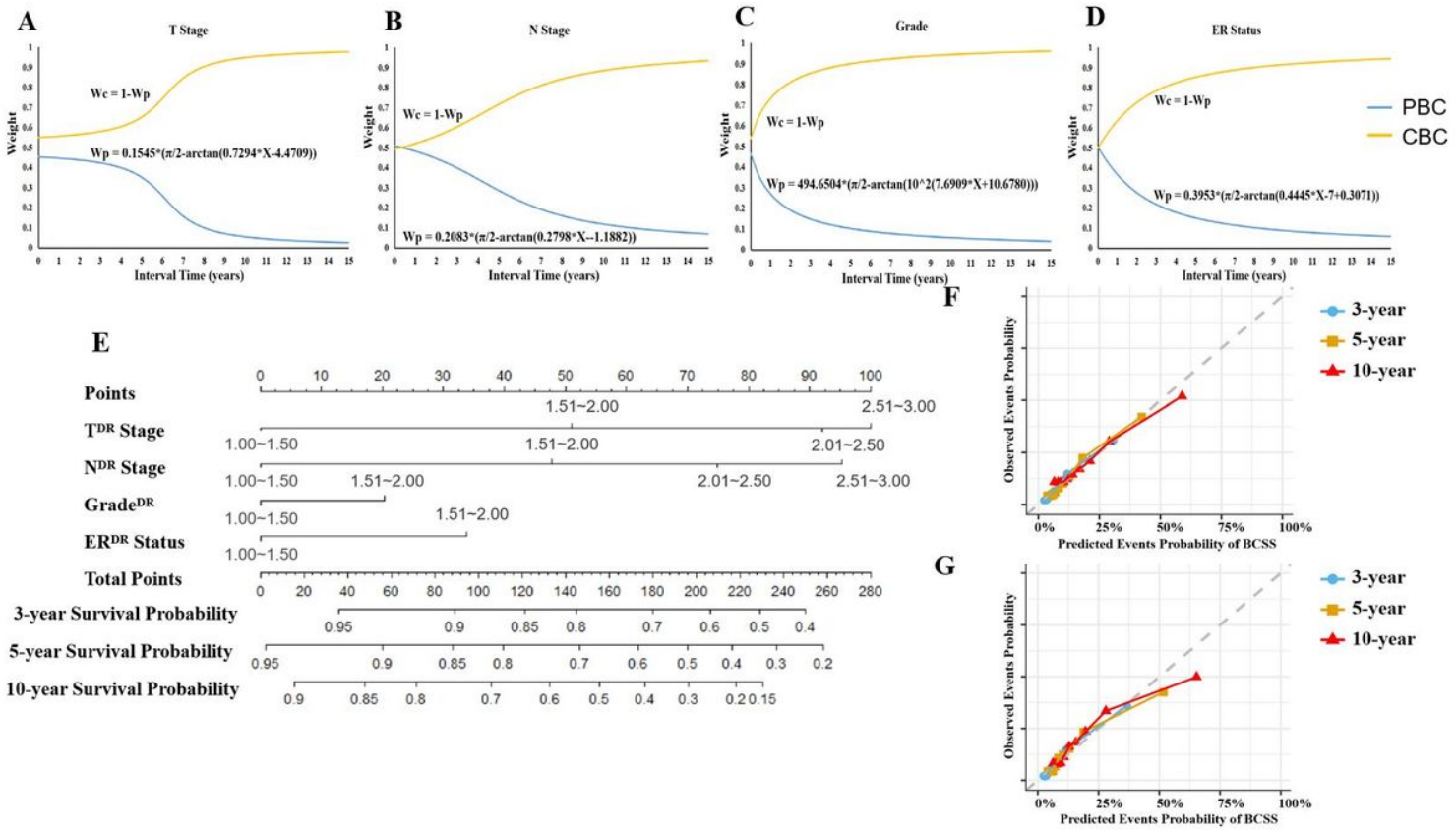

Figure 4

Weight of CIF curves on interval time and DR nomogram (A-D) The weight of T stage (A), N stage (B), grade (C) and ER status (D) belonging to PBC or CBC for prognostic prediction changed with interval time. CIF curves were created to identify the weight of PBC and CBC of the patient with specific interval time when using each character to predict BCCM. Wp: weight of PBC's character. Wc: weight of CBC's character.

Supplementary Files

This is a list of supplementary files associated with this preprint. Click to download.

- Supplementdata.docx
- Supplementtables.docx
- SupplementaryFigure1.pptx
- SupplementaryFigure2.pptx